Theoret. Appl. Mech., Vol. 33, No. 3, pp. 223–243, Belgrade 2006

Wave propagation at the human muscle-compact bone interface

Shao-Yi Hsia * **Shih-Ming Chiu** †
Jyin-Wen Cheng ‡

Abstract

Due to the improvement of the signal processing and image technology, the clinical ultrasound system becomes an important tool to assist doctors in detecting diseases. Hence, it is necessary to know the biological effects of ultrasound in human tissue. In ultrasonic waves, the discrepancy between classic elasticity and experimental elasticity becomes a particularly important problem, especially when there are higher frequencies and smaller wavelengths, i.e., in the case of wave propagation in human muscle and compact bone. Consequently, the influence of the microstructure is important and this fact leads to the generation of new types of waves unknown in classic elasticity. General continuum theories, such as couple stress theory and micropolar theory, have degrees of freedom in addition to those of classic elasticity. Such theories are thought to be applicable to composites with granular or porous structure, effective chiral composite, and human compact bone. In this work, a theoretical analysis concerning the reflected and transmitted fields of an incident plane wave P propagating at the human muscle-compact bone interface has been investigated. The results show that the wave fields are affected by microstructures

*Department of Mechanical Engineering, Yung-Ta Institute of Technology and Commerce, Ping-Tung, 909, Taiwan, R.O.C.

†Department of Mechanical and Electro-Mechanical Engineering, National Sun, Yat-Sen University, Kaohsiung, 804, Taiwan, R.O.C.

‡Cepstrum Technology Corp.Kaohsiung, Taiwan, R.O.C.

of the human bone. Knowledge of this occurrence may offer some contribution to the understanding of the ultrasound propagation in the biological effects of human tissue.

Keywords: Ultrasound, human tissue, microstructures, human compact bone

1 Introduction

The joints of bones are the most commonly injured or diseased parts of the human body. Ultrasonic assessment of bone is applied as radiation-based bone densitometry for managing metabolic disease, especially in Osteo Porosis [1,2]. Ultrasound is a mechanical wave, in contrast to current ionizing electro magnetic radiation-based densitometric methods, and interacts with human bone in a fundamentally distinct manner. Therefore, ultrasound is widely used to diagnose not only bone mass but the architecture and the quality of bone as well [2].

The elastic behavior in bone has been studied by Wertheim and Rauber [3,4] since the nineteenth-century. Many researchers in recent years have demonstrated that bone is anisotropic as well as viscoelastic, and its properties are dependent on direction [5]. Hence, more than two elastic constants are required to describe its behavior. The constitutive equation for an anisotropic solid is

$$\tau_{ij} = c_{ijkl}\varepsilon_{kl}, \tag{1}$$

where $\tau_{ij}$is the symmetric stress tensor, $c_{ijkl}$is the fourth rank elastic modulus tensor, and $\varepsilon_{kl}$is the strain tensor. Since bone is also a natural fibrous composite [6-8], these conventional elasticity theories have a possibility to vary the degree of freedom in bone. Consequently, the couple-stress effects are explored in human compact bone for elastic behavior analysis [7]. Besides, the ultrasonic waves which are generated into the human bone have small wavelengths in comparison with the human tissue. The size effects differences are also considered by couple-stress theory but not by classical elasticity or viscoelasticity [9]. The couple-stress theory, similar to classic force stress elasticity theory, is a continuum representation of the phenomenology of mechanical behavior. It is possible to derive this theory from microstructural or atomistic models as continuum approximations. Much work has been done in microelasticity, couple-stress

theory, and multiple continuum mechanics to incorporate microstructure effects into the continuum theory. Especially, Kroner [10] introduced and developed a general nonlinear theory of micromorphic continua which dealt with the indeterminate couple stress theory and multiple continuum mechanics. This theory is however very complicated. It is perhaps as complicated as comparison in the case of linear elastic solids. To simplify the theory, Eringen recapitulated his works and then introduced the terminology "micropolar elasticity" in his paper [11]. In his research, microstructure is assumed to consist of interconnected particles in the form of small rigid bodies. These small rigid bodies undergo translational and rotational motions when an external force is applied. The constitutive equations may be summarized in Cartesian coordinates as

$$\tau_{ij} = \lambda u_{k,k}\delta_{ij} + \mu(u_{i,j} + u_{j,i}) + \kappa(u_{j,i} - \varepsilon_{ijk}\varphi_k), \tag{2}$$

$$m_{ij} = \alpha\varphi_{k,k}\delta_{ij} + \beta\varphi_{i,j} + \gamma\varphi_{j,i}, \tag{3}$$

where τ_{ij} is the force stress tensor, m_{ij} represent the couple stress tensor, u_i is the displacement, φ_i denotes the microrotation, λ and μ are the Lame's constants and κ, α, β and γ are additional elastic constants associated with micropolar theory. It is a special case, when these discarded in the constitutive equations then the equations of classical elasticity are formed.

When the ultrasonic waves are generated in human bone, the waves propagate as shown in figure 1. The interface between the human muscle and compact bone are assumed to contact completely in the figure 1. A plane wave P, the magnitude is considered as a unit, is applied into the elastic medium with an incident angle θ_1. The material properties of this medium are the mass density ρ_1, Lame's elastic constant λ_1 and μ_1. The reflected waves are also propagated on this plane.

The behavior of micropolar elastic solids have been investigated by several authors [12,13]. Parfitt and Eringen studied the propagation of micropolar elastic waves in an infinite medium and the problems of reflection of plane waves from flat boundaries and free surfaces [12]. In addition, Tomar and Gogna extended these results to discuss the problem of reflection and refraction of a longitudinal microrotational wave at an interface between two micropolar elastic solids [12]. Yang and Hsia in their discussion on wave propagation between elastic-chiral interfaces

have hypothesized the value of the modulus [13]. Furthermore, the classical and Cosserat elastic technical constants of human bone were studied by Lakes et al. through their torsional resonance experiments [7,8,14]. However, few efforts have been made to verify wave propagation between the human muscle-compact bone interface. In this article, we report the microstructure effects and wave fields so as to understand how simulated waves are propagated in bone in the clinical application of ultrasonic techniques.

2 Summary of micropolar theory

The constitutive equation of linear isotropic micropolar elasticity without regarding body forces, and body coupled forces, can be written in the following vector form [11]:

$$(c_1^2 + c_3^2)\nabla(\nabla \bullet \mathbf{u}) - (c_2^2 + c_3^2)\nabla \times (\nabla \times \mathbf{u}) + c_3^2 \nabla \times \boldsymbol{\varphi} = \ddot{\mathbf{u}}, \tag{4}$$

$$(c_4^2 + c_5^2)\nabla(\nabla \bullet \boldsymbol{\varphi}) - c_4^2 \nabla \times (\nabla \times \boldsymbol{\varphi}) + \omega_0^2 \nabla \times \mathbf{u} - 2\omega_0^2 \boldsymbol{\varphi} = \ddot{\boldsymbol{\varphi}}, \tag{5}$$

where

$$c_1^2 = \frac{\lambda + 2\mu}{\rho}, \quad c_2^2 = \frac{\mu}{\rho}, \quad c_3^2 = \frac{\kappa}{\rho}, \quad c_4^2 = \frac{\lambda}{\rho\, J},$$
$$c_5^2 = \frac{\alpha + \beta}{\rho\, J}, \quad \omega_0^2 = \frac{c_3^2}{J} = \frac{\kappa}{\rho\, J}. \tag{6}$$

ρ is the mass density of the material, and J is microinertia.

Decompose the displacement vector u and the microrotation vector φ into scalar and vector potentials as follows

$$\mathbf{u} = \nabla\phi + \nabla \times \boldsymbol{\psi}, \quad \nabla \bullet \boldsymbol{\psi} = 0, \tag{7}$$

$$\boldsymbol{\varphi} = \nabla\zeta + \nabla \times \mathbf{H}, \quad \nabla \bullet \mathbf{H} = 0. \tag{8}$$

Substituting (7) and (8) into the equations of motion (4) and (5), we obtain the equations

$$(c_1^2 + c_3^2)\nabla^2\phi = \ddot{\phi}, \tag{9}$$

$$(c_4^2 + c_5^2)\nabla^2\zeta - 2\omega_0^2\zeta = \ddot{\zeta}, \tag{10}$$

$$(c_2^2 + c_3^2)\nabla^2\boldsymbol{\psi} + c_3^2\nabla \times \mathbf{H} = \ddot{\boldsymbol{\psi}}, \tag{11}$$

$$c_4^2\,\nabla^2\mathbf{H} + \omega_0^2\,\nabla \times \boldsymbol{\psi} - 2\omega_0^2\mathbf{H} = \ddot{\boldsymbol{\psi}}. \tag{12}$$

Assume that the plane waves travel in an infinite micropolar elastic medium, there are four basic waves traveling with different phase velocities. These are as follows:

$$V_1 = \frac{\omega}{k_1} = \sqrt{\frac{\lambda + 2\mu + \kappa}{\rho}}, \tag{13}$$

$$V_2 = \frac{\omega}{k_2} = \sqrt{\frac{\alpha + \beta + \gamma}{\rho\, J(1 - 2\omega_0^2/\omega^2)}}, \tag{14}$$

$$\begin{aligned} V_{3,4}^2 = \tfrac{1}{2(1-x)}\Bigg[& C_4^2 + C_3^2 + C_2^2 - \left(C_2^2 + \tfrac{1}{2}C_3^2\right)x \pm \\ & \left\{\left[(C_4^2 - C_2^2 - C_3^2) + \left(C_2^2 + \tfrac{1}{2}C_3^2\right)x\right]^2 + 2C_3^2C_4^2x\right\}^{\frac{1}{2}}\Bigg], \end{aligned} \tag{15}$$

where $x = 2\omega_0^2/\omega^2$. V_1 is the phase velocity of longitudinal displacement plane waves, V_2 is the phase velocity of longitudinal microrotation plane waves, V_3 and V_4 are two coupled sets of the phase velocity that consist of the transverse displacement waves and the transverse microrotation waves.

3 Wave fields for human muscle and compact bone media

Let the plane longitudinal wave be incident on the plane boundary $z = 0$ that separates human muscle 1 and human compact bone 2, and as shown in Figure 1. The plane of incidence of the wave is coincident with the xz-plane and therefore

$$\mathbf{u} = u_1\,\mathbf{i} + u_3\,\mathbf{k}, \tag{16}$$

$$\boldsymbol{\varphi} = \varphi_2\,\mathbf{j}, \tag{17}$$

with $u_2 = 0, \varphi_1 = 0, \varphi_3 = 0$ and $\partial/\partial y = 0$. In this figure, the material properties of the human muscle 1 where the incident and the reflected waves propagate are ρ_1, λ_1 and μ_1. The material constants of the human compact bone 2 for transmission waves are ρ_2, λ_2, μ_2, κ, α, β, γ and J.

It should be noted that the micropolar medium contains a longitudinal microrotation plane wave (denoted by $P1$), and two sets of coupled transverse displacement and transverse microrotation waves (denoted by $S3$ and $S4$). To satisfy the boundary conditions at the human muscle-compact bone interface, it is necessary to postulate that the longitudinal microrotation wave is discarded. Consequently, a plane wave incident from the upper half-space ($z < 0$) of the compact bone generates the $P1$, $S3$, and $S4$ waves. The incident P wave can be represented with the displacement potential in the form

$$\phi^{I1} = \phi^{I} \ \exp\left[i\, k_L \left(x \sin\theta_1 + z \cos\theta_1\right)\right]. \tag{18}$$

For the reflected P and SV waves, we have

$$\phi^{R1} = \phi^{R} \exp\ \left[i\, k_L \left(x \sin\theta_2 - z \cos\theta_2\right)\right], \tag{19}$$

$$\boldsymbol{\psi}^{R1} = \mathbf{j}\psi^{R}\ \exp\left[i\, k_s \left(x \sin\theta_3 - z \cos\theta_3\right)\right]. \tag{20}$$

Similarly, the transmitted $P1$, $S3$, and $S4$ waves in the lower half-space ($z > 0$) are

$$\phi^{T2} = \phi^{T}\ \exp\left[i\, k_1 \left(x \sin\theta_1 + z \cos\theta_1\right)\right], \tag{21}$$

$$\boldsymbol{\psi}^{T2} = \mathbf{j}\ \psi^{T}_{qy} \exp\left[i\, k_q \left(x \sin\alpha_q + z \cos\alpha_q\right)\right], \quad q = 3, 4, \tag{22}$$

$$\mathbf{H}^{T2} = \left(H^{T}_{qx}\, \mathbf{i} + H^{T}_{qz}\, \mathbf{k}\right) \exp\left[i\, k_q \left(x \sin\alpha_q + z \cos\alpha_q\right)\right] \quad q = 3, 4, \tag{23}$$

where ϕs, ψs and Hs are the amplitudes of the propagation waves determined by the boundary conditions, θs are the incident angle and reflected angle, αs are the transmitted angles, ks are wave numbers (k_1 corresponds to $P1$, k_3 corresponds to $S3$, and k_4 corresponds to $S4$) , and i, j, k are the Cartesian unit vectors. The time dependence ($e^{-i\omega t}$) has been suppressed. For a further convenience in identification, the fields associated with the incident wave are denoted by the superscript "$I1$", those with the reflected wave by "$R1$", and those with the transmitted waves by "$T2$". Since the vectors ψ and H are perpendicular to each other, they

are coupled and cannot exist individually. Thus, the following relations are to hold:

$$H_{qx}^{T} = ik_q \cos\alpha_q \Delta_q \psi_{qy}^{T}, \tag{24}$$

$$H_{qz}^{T} = -ik_q \sin\alpha_q \Delta_q \psi_{qy}^{T}, \tag{25}$$

where

$$\Delta_q = \frac{\kappa}{\omega^2 \rho_2 J - \gamma \kappa_q^2 - 2\kappa}. \tag{26}$$

The nonvanishing components of the stress-displacement and the couple-stress-rotation relations are

$$\tau_{33} = \lambda\,(u_{1,1} + u_{3,3}) + (2\mu + \kappa) u_{3,3}, \tag{27}$$

$$\tau_{31} = \mu\,(u_{3,1} + u_{1,3}) + \kappa(u_{1,3} - \varphi_2), \tag{28}$$

$$m_{32} = \beta\,\varphi_{3,2} + \gamma\,\varphi_{2,3}. \tag{29}$$

Six boundary conditions are obtained from the behavior of the wave continuity for the components of the displacement u, the rotation φ, the stress τ and the coupled-stress m at $z = 0$. This yields

$$u_1^{I1} + u_1^{R1} = u_1^{T2}, \quad u_3^{I1} + u_3^{R1} = u_3^{T2}, \quad \varphi_2^{I1} + \varphi_2^{R1} = \varphi_2^{T2}, \tag{30}$$

and

$$\tau_{33}^{I1} + \tau_{33}^{R1} = \tau_{33}^{T2}, \quad \tau_{31}^{I1} + \tau_{31}^{R1} = \tau_{31}^{T2}, \quad m_{32}^{I1} + m_{32}^{R1} = m_{32}^{T2}. \tag{31}$$

By substituting (7) and (8) into (27)-(29), the stresses may be written of the potentials. Then, with a combination of the boundary conditions (30) and (31), we arrive at the six equations as follows

$$\begin{aligned}&(-k_L \sin\theta_3)\phi^R - (k_s \cos\theta_4)\psi_y^R + (k_1 \sin\alpha_1)\phi^T - \\ &(k_3 \cos\alpha_3)\psi_{3y}^T - (k_4 \cos\alpha_4)\psi_{4y}^T = (k_L \sin\theta_1)\phi^I,\end{aligned} \tag{32}$$

$$\begin{aligned}&(k_L \cos\theta_3)\phi^R - (k_s \sin\theta_4)\psi_y^R + (k_1 \cos\alpha_1)\phi^T + \\ &(k_3 \sin\alpha_3)\psi_{3y}^T + (k_4 \sin\alpha_4)\psi_{4y}^T = (k_L \cos\theta_1)\phi^I,\end{aligned} \tag{33}$$

$$k_3^2 \Delta_3 \psi_{3y}^T + k_4^2 \Delta_4 \psi_{4y}^T = 0, \tag{34}$$

$$
\begin{aligned}
&-(\lambda+2\mu\cos^2\theta_3)k_L^2\phi^R+(\mu\sin 2\theta_4)k_s^2\psi_y^R+\\
&[\lambda_2+(2\mu_2+\kappa)\cos^2\alpha_1]k_1^2\phi^T+(2\mu_2+\kappa)\\
&(\sin\alpha_3\cos\alpha_3)k_3^2\psi_{3y}^T+(2\mu_2+\kappa)\\
&(\sin\alpha_4\cos\alpha_4)k_4^2\psi_{4y}^T=(\lambda+2\mu\cos^2\theta_1)k_L^2\phi^I,
\end{aligned}
\tag{35}
$$

$$
\begin{aligned}
&(\mu\sin 2\theta_3)k_L^2\phi^R+(\mu\cos 2\theta_4)k_s^2\psi_y^R+(2\mu_2+\kappa)\\
&(\sin\alpha_1\cos\alpha_1)k_1^2\phi^T-(\mu_2\cos 2\alpha_3+\kappa\cos^2\alpha_3+\kappa\,\Delta_3)k_3^2\psi_{3y}^T-\\
&(\mu_2\cos 2\alpha_4+\kappa\cos^2\alpha_4+\kappa\,\Delta_4)k_4^2\psi_{4y}^T=(\mu\sin 2\theta_1)k_L^2\phi^I,
\end{aligned}
\tag{36}
$$

$$
k_3^3(\cos\alpha_3)\Delta_3\psi_{3y}^T+k_4^3(\cos\alpha_4)\Delta_4\psi_{4y}^T=0. \tag{37}
$$

To solve five unknowns $\{\phi^R,\ \psi_y^R,\ \phi^T,\ \psi_{3y}^T,\ \psi_{4y}^T\}$ at the human muscle-compact bone interface, only five boundary conditions are needed. To simplify the analysis, the boundary condition A is defined by equations (32)-(36), and the boundary conditions B by equations (32)-(33), and (35)-(37). These two sets of conditions are discussed in the remainder of the paper.

Since the energy flux will be conserved at the interface, the energy of the incident waves must equal the sum of the energies of the reflected and transmitted waves. The energy flux (energy per unit time per unit area) at $z=0$ is given by

$$
P=\tau_{31}\dot{u}_1+\tau_{33}\dot{u}_3+m_{32}\dot{\varphi}_2, \tag{38}
$$

where $\dot{u}_i=\partial u_i/\partial t \quad (i=1,\,3)$, $\dot{\varphi}_2=\partial\phi_2/\partial t$.

Therefore, the energy flux for the incident longitudinal waves is

$$
P_p^I=-(\lambda+2\mu)(\cos\theta_1)\,\omega\,k_L^3(\phi^I)^2. \tag{39}
$$

The energy flux for the reflected longitudinal wave and transverse waves are

$$
P_p^R=(\lambda+2\mu)(\cos\theta_3)\,\omega\,k_L^3(\phi^R)^2, \tag{40}
$$

$$
P_{sv}^R=\mu(\cos\theta_4)\,\omega\,k_s^3(\psi_y^R)^2. \tag{41}
$$

The energy flux for the transmitted longitudinal wave and transverse wave are

$$P_{p1}^{T} = -(\lambda_2 + 2\mu_2 + \kappa)(\cos\alpha_1)\,\omega\, k_1^3(\phi^T)^2, \tag{42}$$

$$P_{s3}^{T} = -(\mu_2 + \kappa + \kappa\,\Delta_3 + \gamma\, k_3^2\Delta_3^2)(\cos\alpha_3)\,\omega\, k_3^3(\psi_{3y}^T)^2, \tag{43}$$

$$P_{s4}^{T} = -(\mu_2 + \kappa + \kappa\,\Delta_4 + \gamma\, k_4^2\Delta_4^2)(\cos\alpha_4)\,\omega\, k_4^3(\psi_{4y}^T)^2, \tag{44}$$

where the superscripts R and T of P denote the reflected and transmitted fields, respectively, the subscripts P and SV represent the reflected waves, and $P1$, $S3$, and $S4$ represent the transmitted waves.

There is no dissipation of energy during transmission. We have the energy ratio E:

$$1 = \frac{P_p^R}{P_p^I} + \frac{P_{sv}^R}{P_p^I} + \frac{P_{p1}^T}{P_p^I} + \frac{P_{s3}^T}{P_p^I} + \frac{P_{s4}^T}{P_p^I} \; = E_p^R + E_{sv}^R + E_{p1}^T + E_{s3}^T + E_{s4}^T. \tag{45}$$

4 Numerical results and discussion

The material properties of the elastic medium 1 are obtained from the human muscle: longitudinal wave velocity $V_L = 1560m/sec$ and density $\rho = 1074kg/m^3$. Results for the mechanical properties of the human compact bone, as obtained by several authors, are as follows in reference 7 and 8 that were obtained from donated fresh-frozen autopsy tissue. They are consistent with the following results: Young's modulus $E = 12GPa$, shear modulus $G = 4.2MPa$, characteristic length of torsion $l_t = 0.22mm$, characteristic length of bending $l_b = 0.45mm$, coupling number $N^2 = 0.3844$ and polar ratio $\xi = 1.5$. Consequently, the mechanical elastic constants of medium 2 are found to yield through the formulas $E = (2\mu + \kappa)\,(3\lambda + 2\mu + \kappa)\,/\,(2\lambda + 2\mu + \kappa)$, $G = (2\mu + \kappa)\,/2$, $l_t = [(\beta + \gamma)\,/\,(2\mu + \kappa)]^{1/2}$, $l_b = [\gamma/2\,(2\mu + \kappa)]^{1/2}$, $N = [\kappa/2\,(\mu + \kappa)]^{1/2}$ and $\xi = (\beta + \gamma)\,/\,(\alpha + \beta + \gamma)$.

Hence, the material constants of the human bone can be obtained by substituting the formulas and listed them in Table 1. The variation of the microinertia with the cut off frequency is shown in figure 2 for human compact bone. Figure 2 represents the cut off frequency which is calculated by $\sqrt{2}\,\omega_0 = \omega_c$ for the wave's propagation of refracted coupled wave $S3$. The set of coupled waves $S3$ traveling at speed V_3 propagates

only if $\omega > \omega_c$ is found degenerating into a distance decaying sinusoidal vibration otherwise. Hence, the excited frequency should be higher than the cut off frequency in interested microinertia, and then the refracted coupled transverse waves are found to have a possible propagation $S3$ in the human compact bone. It is noted in figure 2 for the lower value of the microinertia that the cut off frequency is almost infinite, which means it is difficult to generate the transverse wave $S3$ at the higher frequency. For this reason, the range from 0.15×10^{-6} to 2.0×10^{-6} m^2 of the microinertia is investigated herein for the longitudinal plane wave incident from human muscle to human compact bone. Since the longitudinal plane wave is a nondispersive propagating wave, the phase velocities are independent of frequency. The transmitted longitudinal plane wave $P1$ is hence a nondispersive propagating wave shown as figure 3, and the considered ranges (0.15×10^{-6} to 2.0×10^{-6} m^2) of the microinertia vary linearly with the wave number.

Although the refracted transverse waves $S3$ and $S4$ are dispersive, the wave number of the $S4$ wave is almost linear in frequency in human compact bone as shown in figure 4(b). In contrast to the $S4$ wave, the wave number of the $S3$ wave shown in figure 4(a) has a large distinction at lower frequency. So, the phase velocity of the $S3$ wave is dependent on frequency at lower frequency. It should be noted that there is an increase in wave number for the $S3$ wave from 0.15×10^{-6} to 0.49×10^{-6} m^2 of the microinertia, and it is a constant wave number above the value 0.49×10^{-6} m^2 of the microinertia. In figure 4, both of the $S3$ wave and the $S4$ wave have a greater variation for $J = 0.49 \times 10^{-6}$ m^2, which is calculated by $\gamma/J \geq \mu + \kappa$ due to a consistent solution (15). It represents what has been found that the $S3$ wave and the $S4$ wave may have some interesting phenomenon at the specified value of microinertia.

According to the phenomenon mentioned above, the reflected longitudinal wave P always has some variations when the value of microinertia is near 0.49×10^{-6} m^2 as shown in figure 5. The energy ratio of reflected longitudinal wave P begins the fixed value when $\theta_1 = 0^\circ$. It has maximum value at $\theta_1 = 22^\circ$ due to the grazing transmitted $P1$ wave and the other maximum value when incident angle is above 54^o due to the grazing transmitted $S4$ wave. In the refracted field, the longitudinal plane wave $P1$ is generated below the incident angle 22^o. From the profiles shown in figure 6, the energy ratio of $P1$ also exists with a fixed value when $\theta_1 = 0^\circ$.

The energy ratio of $P1$ doesn't exhaust until the incident angle is found increasing to $\theta_1 = 22°$. The phenomenon of the grazing transmitted $P1$ wave is known as the Rayleigh-Wood anomalies. This consequence may imply that it is possible for doctors to detect diseases on human bone using ultrasonic assessment below the incident angle 22°. The $S3$ wave as shown in figure 7 has the maximum value on the microinertia above $0.49 \times 10^{-6}\ m^2$, which increase quickly and then have a fixed value when microinertia is found to be greater. At the same time, the influence of the $S3$ wave will vanish gradually when the incident angle is above $\theta_1 = 50°$ or microinertia is lower than $0.49 \times 10^{-6}\ m^2$. It is interesting to see in figure 8, that the $S4$ wave can be transmitted in unexpected ranges of the microinertia. The transverse field is obviously dominated by the $S4$ wave from $\theta_1 = 22°$ to 53°. Hence, in the case of wave propagation in human muscle and compact bone, the $S4$ wave has a significant micropolar effect on the interface if only $J \leq 0.49 \times 10^{-6}\ m^2$ used. The results of these figures show that the wave propagation in the considered ranges will obey the Snell's law between the incident-reflected and transmitted plane waves.

The wave propagation at the interface between human muscle, and human compact bone, is different from the classic case. Two sets of boundary conditions, A and B, are necessary to find the unknown coefficients. The numerical results have been done for a propagating wave at the chiral-chiral interface by Lakhtakia *et al.* [13,16]. They indicated that a great distinction was obtained for simulation between boundary conditions A and B. This naturally leads to the problem of the difference in the two kinds of boundary conditions during wave propagating in the case of human muscle-compact. Hence, the case of the wave propagation on the human muscle-compact bone is the other interesting topic, and will be mentioned below. In this study, take the case of $J = 0.4 \times 10^{-6}\ m^2$ for example it is shown that the numerical results of oblique incidence on the human muscle-compact bone interface for boundary conditions A and B at 4 MHz in figure 9. The results show that a normal incidence is implied, and hence no mode conversion occurs in the two cases, because the longitudinal plane wave incident on the interface generates only the reflected and transmitted longitudinal plane waves. By comparison, the results in figure 9 (a) and (b), the profiles of energy ratio P_{p1}^{T} are nearly the same as the results for boundary conditions A and B. The normal-

ized energy ratio of the $S3$ and $S4$ waves will be the grazing transmitted transverse waves when incident angle are above 43.5^o and 53^o respectively for both boundary conditions A and B as shown as figure 9. Both of the cases show that $S4$ will dominate the transmitted field. The consequence is similar with the phenomena shown in Figs.7 and 8. It becomes evident that the use of boundary condition A or B can lead to the different consequence presented in the reflected and refracted field. The conclusion is the same when compared with the wave propagation at the achiral-chiral interface based on the results of Lakhtakia *et al.* In general, different coupled transverse waves $S3$ or $S4$ will dominate the wave fields according to which value of microinertia we are looking at.

5 Conclusions

The wave propagation that occurs in the human muscle-compact bone has been examined in this study. The unbalance of energy is observed for the specified region of microinertia, and hence only the suitable values can be used to know the phenomenon of wave propagation that occurs in human compact bone. This consequence leads us to induce that the wave fields will be affected by the critical value of microinertia, especially the transmitted transverse waves $S3$ and $S4$. Above the critical value of microinertia, only the $S3$ wave can transmit in the human compact bone. Below that, the $S4$ dominates the wave fields that contain all the reflected and transmitted plane waves. The simulated result also indicates that there are some significant distinctions in the reflection and transmission characteristics from the two sets of boundary condition for a variety incident angle. Knowledge of this occurrence leads us to imply that it is possible to solve the wave response by using the micropolar structural theory, and hence can be referred to the understanding of the ultrasound propagation in biological effects of human tissue.

Acknowledgments This investigation was supported in part by the National Science Council of Taiwan, Republic of China, through grant NSC 94-2212-E-132-002.

References

[1] D. Hans, A. M. Schott and P.J. Meunier, *Ultrasonic assessment of bone: a review*, Eur. J. Med., **2**(3), (1993), 157-163.

[2] J. J. Kaufman, T.A. Einhorn, *Perspective: ultrasound assessment of bone*, J.Bone. Miner Res., **8**(5), (1993), 517-525.

[3] G. Wertheim, *Memoire Sur Elasticite et la Cohesion des principaux Tissus du Corps Human*, Ann de Chirn et de Phys., **21**, (1847), 385-414.

[4] A. A. Rauber: *Elasticitat und Festigkeit der Knochen*, Anatomisch-Physiologische Studie, (1876).

[5] W. T. Dempster and R. T. Liddicoat, *Compact bone as a non-isotropic material*, American Journal of Anatomy, **91**, (1952), 331-362.

[6] R. S. Lakes, H. S. Yoon and J. L. Katz, *Ultrasonic wave propagation and attenuation in wet bone*, J. Biomed Eng., **8**, (1986), 143-148.

[7] R. S. Lakes, *Dynamical study of couple stress effects in human compact bone*, Trans. ASME, **104**, (1982), 6-11.

[8] J. F. C. Yang and R. S. Lakes, *Experimental study of micropolar and couple stress elasticity in compact bone in bending*, J. Biomechanics, **15**, (1982), 91-98.

[9] R. D. Mindlin and H. F. Tiersten, *Effects of couple-stress in linear elasticity*, Archive for Rational Mechanics and Analysis, **11**, (1962), 415-448.

[10] E. Kroner, *Mechanics of Generalized Continua*, Springer-Verlag, Berlin, 1968.

[11] A.C. Eringen, *Theory of micropolar elasticity*, Fracture: A Treatise, Vol.2, H. Liebowitz (ed.), p.621; Academic Press, New York, 1968.

[12] S. K. Tomar and M. L. Gogna, *Reflection and refraction of longitudinal microrotational wave at aniinterface between two micropolar elastic media in welded contact,*, Int. J. Eng. Sci., **30**, (1992), 1637-1646.

[13] S.Y. Hsia and J.W. Cheng, *Longitudinal plane wave propagation in elastic-micropolar porous media*, Jpn. J. Appl. Phys., **45(3A)**, (2006), 1743-1748.

[14] V.R. Parfitt and A.C. Eringen, *Reflection of plane waves from the flat boundary of a micropolar elastic half-space*, J. Acoust. Soc. Am. (JASA), **45/5**, (1969), 1258-1272.

[15] P.M. Buechner and R.S. Lakes, *Size effects in the elasticity and viscoelasticity of bone*, Biomechan Model Mechanobiol, **1**, (2003), 295-301.

[16] S. K. Tomar and M. L. Gogna, *Reflection and refraction of longitudinal wave at an interface between two micropolar elastic solid in welded contact*, J. Acoust. Soc. Am. (JASA), **97/2**, (1995), 822-830.

[17] A. Lakhtakia, V. K. Varadan and V. V. Varadan, *Reflection of elastic plane waves at a planar achiral-chiral interface*, J. Acoust. Soc. Am. (JASA), **87/6**, (1990), 2314-2318.

Human muscle	Human compact bone
$\rho_1 = 970kg/m^3$	$\rho_2 = 1012kg/m^3$
$\lambda_1 = 2289.22MPa$	$\lambda_2 = 2124.7Mpa$
	$\mu_2 = 1.58\ MPa$
	$\alpha = 3 \times 10^6 N$
	$\beta = 3 \times 10^6 N$
	$\gamma = 4 \times 10^6 N$
	$C_3 = 16 \times 10^6 Nm^{-1}$
	$J = 0.01m^2$

Table 1: The material constants of human muscle and compact bone

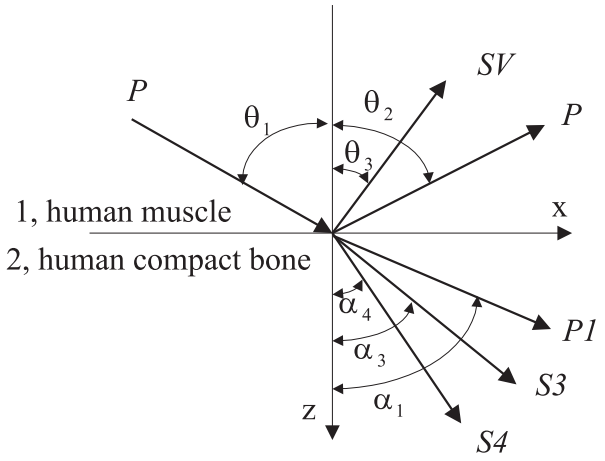

Figure 1: Reflection and transmission of the incident longitudinal plane wave; plane 1 is the human muscle, and plane 2 represents the human compact bone.

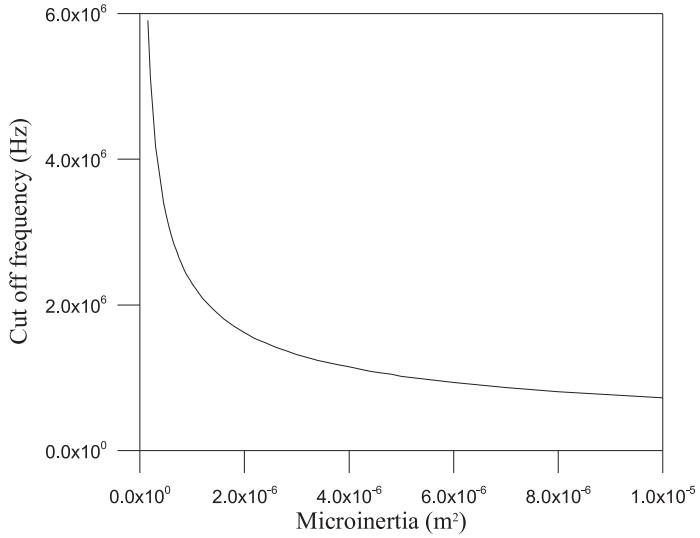

Figure 2: Cut off frequency as functions of the microinertia

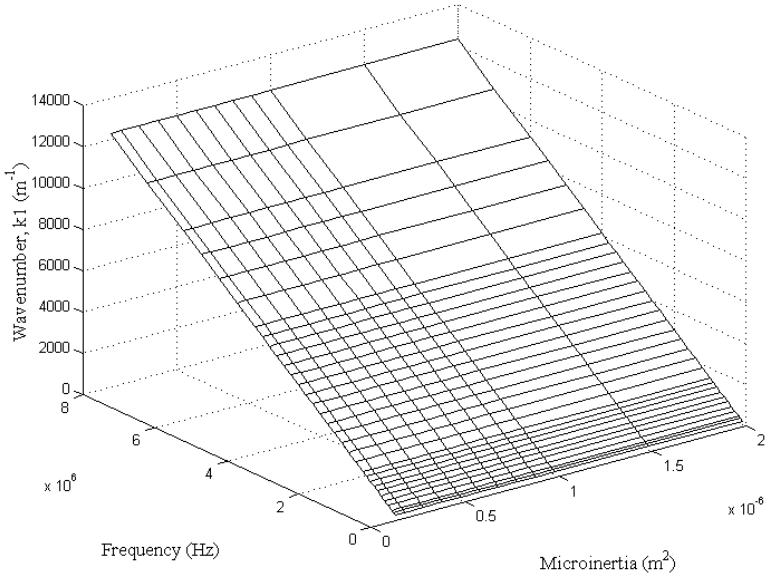

Figure 3: Wave numbers of $P1$ as functions of frequency and microinertia.

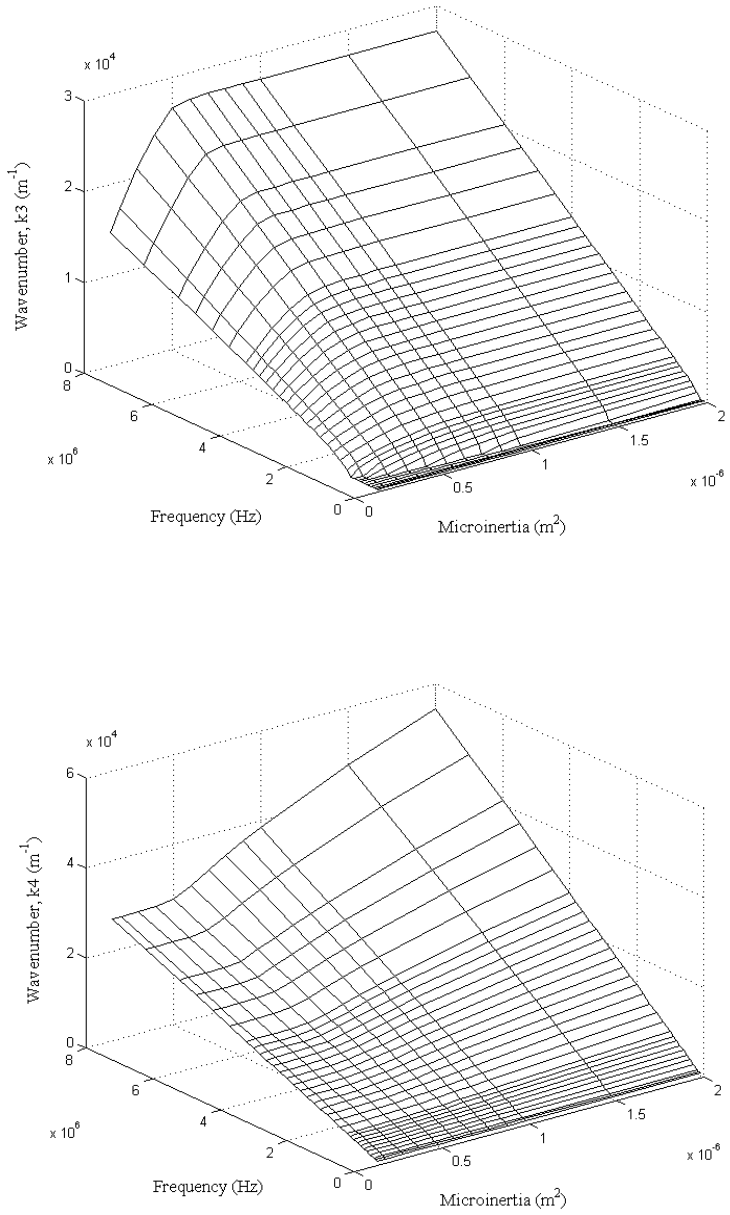

Figure 4: Wave numbers of $S3$ and $S4$ coupled waves as functions of frequency and microinertia: (a) $S3$ wave, (b) $S4$ wave

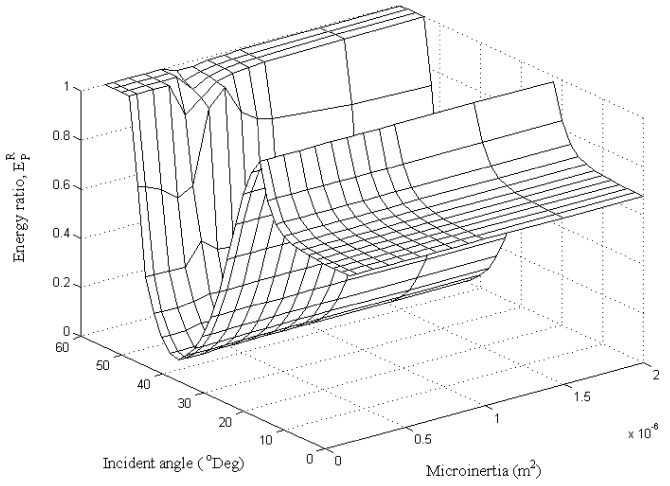

Figure 5: The energy ratio of reflected P wave as functions of incident angle and microinertia.

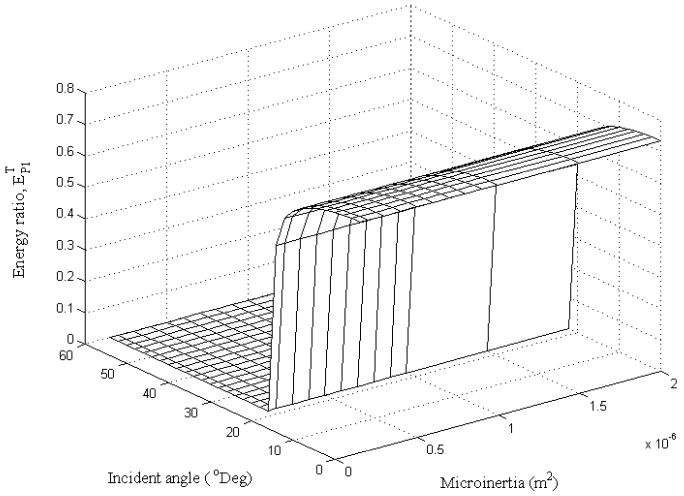

Figure 6: The energy ratio of transmitted $P1$ wave as functions of incident angle and microinertia.

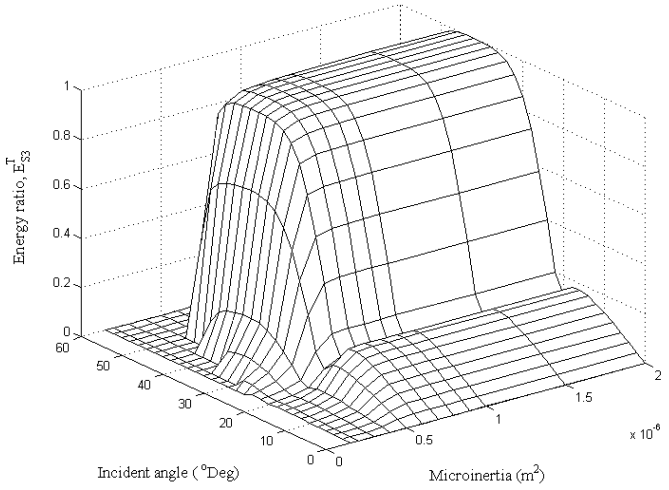

Figure 7: The energy ratio of transmitted $S3$ wave as functions of incident angle and microinertia.

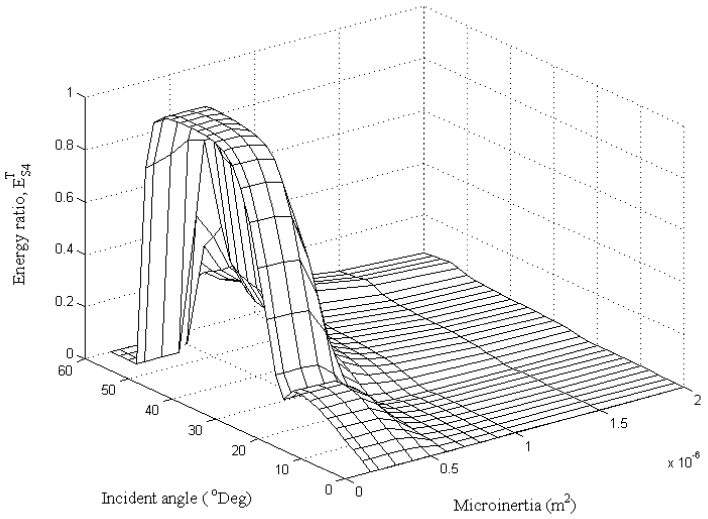

Figure 8: The energy ratio of transmitted $S4$ wave as functions of incident angle and microinertia.

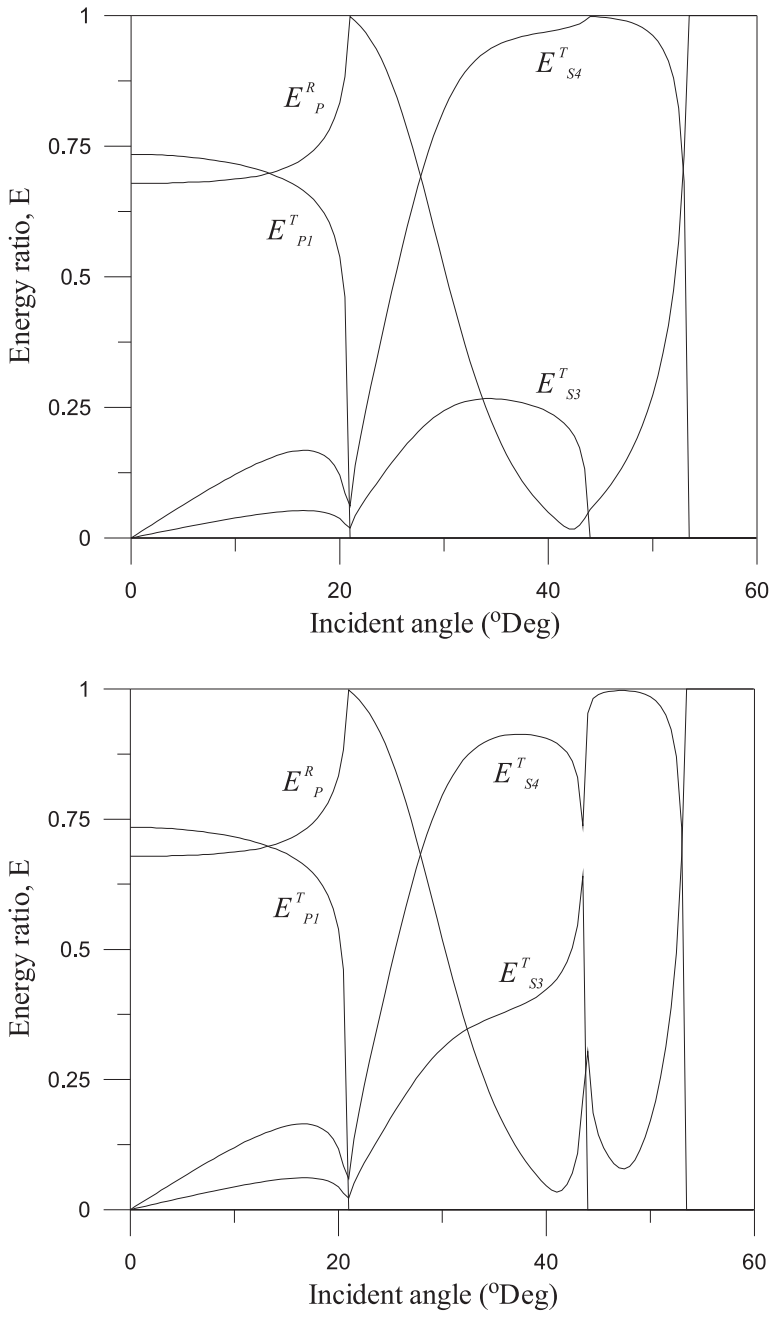

Figure 9: The energy ratio of wave fields at $J = 0.4 \times 10^{-6} m^2$ for 4 MHz: (a) boundary conditions A, (b) boundary conditions B.

Submitted on November 2006.

Prostiranje talasa na medjupovrši ljudskog mišića i kompaktne kosti

UDK 534.16

Zahvaljujući progresu tehnologije procesiranja signala i slika, klinički ultrazvučni sistem je postao značajan pomoćni alat lekarima pri dijagnostici bolesti. Dakle, potrebno je poznavati biološke efekte ultrazvuka u ljudskom tkivu. Kod ultrazvučnih talasa razlika izmedju klasične i eksperimentalne elastičnosti postaje posebno značajan problem pogotovu pri višim učestanostima i manjim talasnim dužinama - što znači u slučaju prostiranja talasa u ljudskom mišiću i kompaktnoj kosti. Prema tome, uticaj mikrostrukture je značajan i ova činjenica vodi ka generaciji novih tipova talasa nepoznatih u klasičnoj elastičnosti. Opšte teorije kontinuuma, kao teorija naponskih spregova i mikropolarna teorija, imaju dopunske stepene slobode u odnosu na klasičnu elastičnost. Za takve teorije se smatra da su primenjive na kompozite sa zrnastom i poroznom strukturom, efektivno hiralne kompozite kao i ljudsku kompaktnu kost. U ovom radu izvodi se teorijska analiza odbijenih i propuštenih talasa jednog ulaznog ravanskog P-talasa. Rezultati pokazuju da na talasna polja utiče mikrostruktura ljudske kosti. Poznavanje ove pojave može da ponudi doprinos razumevanju ultrazvučnog prostiranja u tkivu ljudske kosti.